Polymer 158 (2018) 354–363

Contents lists available at ScienceDirect

Polymer

journal homepage: www.elsevier.com/locate/polymer

Effect of chemical structure on thermo-mechanical properties of epoxy polymers: Comparison of accelerated ReaxFF simulations and experiments

Aniruddh Vashisth[a], Chowdhury Ashraf[b], Charles E. Bakis[a], Adri C.T. van Duin[a,b,*]

[a] Department of Engineering Science and Mechanics, The Pennsylvania State University, 212 Earth-Engineering Sciences Building, University Park, PA, 16802, USA
[b] Department of Mechanical Engineering, The Pennsylvania State University, 136 Research East Building, Bigler Road, University Park, PA, 16802, USA

HIGHLIGHTS

- Accelerated reactive molecular dynamics simulations for kinetically slow reactions to examine crosslinking in epoxies with different amines.
- The method was able to simulate crosslinking of bisphenol-A epoxide with three different amine curing agents.
- Thermo-mechanical properties of simulated polymers show agreement with experimental results.
- Cyclic curing agents show higher local heterogeneities, while strain rate dependence is manifested prominently in aliphatic curing agents.

ARTICLE INFO

Keywords:
Molecular dynamics
ReaxFF
Simulations

ABSTRACT

Chemical structure governs the bulk material properties of thermoset polymers at the macro-scale. In this study, three different amine curing agents — aromatic, cyclo-aliphatic and aliphatic — are reacted with bisphenol-A epoxide using a recently developed accelerated ReaxFF simulation approach for kinetically slow reactions. Accelerated ReaxFF simulations provide reactants with energy (comparable to the barrier energy) to form a stable transition state that, depending upon the proximity and the path of approach, leads to successful cross-linking. While cyclic curing agents result in simulated polymers with local heterogeneities in the molecular structure that can be resolved by annealing, strain rate dependence is manifested prominently in polymers with aliphatic curing agents and less prominent in polymer with aromatic curing agent. Based on the good correlation obtained between simulations and experiments, this work demonstrates that accelerated cross-linking and virtual testing of the polymer can capture the translation of variable chemical structure to thermo-mechanical properties of thermosets.

1. Introduction

Epoxy polymers are widely used in engineering applications requiring high stiffness and strength. Epoxies for specific applications are selected based on their thermo-mechanical properties that, in turn, depend on polymer chemistry and molecular structure [1]. Cross-linking of the molecular structure can be altered by various factors such as processing conditions, whereas polymer chemistry can be changed by using different stoichiometric ratios of amine and epoxide, as well as different combinations of epoxides and amine curing agents [2–5]. Selecting suitable polymers with appropriate properties for specific applications could require extensive experimentation. However, the number of experiments can be minimized by short-listing viable material candidates based on molecular simulations. Molecular dynamics has been used to simulate the thermo-mechanical properties of epoxies through virtual testing [6–9] and therefore can be used to assess the suitability of a polymer for a particular application.

Simulating the cross-linking of epoxy is a challenging task, as thermoset polymers polymerize to roughly 75–80% cross-link density over time periods of a few minutes to several days. Such simulations are computationally very expensive and practically impossible with the current state-of-the-art computational power. To overcome this barrier, various methods have been proposed such as coarse grain molecular simulations [10,11], kinetic Monte Carlo methods that are dependent on transition state rate-kinetics [12], and cut-off distance methods where the distances between the reactive sites in the participating molecules are monitored and bonds are manufactured when the reactive sites are in close range [13–15]. Other methods have also been

* Corresponding author. Department of Engineering Science and Mechanics, The Pennsylvania State University, 212 Earth-Engineering Sciences Building, University Park, PA, 16802, USA.
E-mail address: acv13@psu.edu (A.C.T. van Duin).

https://doi.org/10.1016/j.polymer.2018.11.005
Received 11 August 2018; Received in revised form 23 October 2018; Accepted 3 November 2018
Available online 04 November 2018
0032-3861/

developed that involve single step polymerization [6], activated reactive sites using a cut-off method [7,8] and a cross-linking scheme based on an electronegativity equalization method [16]. While these cross-linking mechanisms capture the dependence of the reaction on the proximity of the reactive sites, they are not able to evaluate the complete reaction path that involves the transition state of the reactants. Reactive force fields, such as Reactive Empirical Bond Order (REBO) and ReaxFF [17–19] are required to atomistically simulate chemical reactions, thereby providing a deeper understanding of the reaction pathway as well as post-processing of the polymer. While variable epoxide monomers cross-linked by cut-off distance affect the polymer properties [20], the percentage cross-linking of the polymers also depends on the monomer chemistry.

To replicate the polymerization process, we recently established a new cross-linking method within the ReaxFF framework – "Accelerated ReaxFF." Accelerated ReaxFF takes into account the barrier energy, the distance between the reacting molecules and the approach of molecules leading up to the reaction [21]. While some previous studies activated the reactive sites by breaking CH_2—O bonds in epoxides and N—H bonds in amine curing agents [7,8], such activation is not required for accelerated ReaxFF. Also, unlike kinetic Monte Carlo (kMC) [12], accelerated ReaxFF does not require precise transition state rate constants but accounts for local variations caused by steric hindrance or a catalyst present in the system. Using accelerated ReaxFF, the effect of molecular chemistry can be analyzed, specifically in terms of amine curing agents. In this investigation, bisphenol A epoxides are cured with three different types of curing agents – aromatic, cycloaliphatic and aliphatic primary amines – and then tested virtually and experimentally for different thermo-mechanical properties. The polymers were virtually tested for density, glass transition temperature, coefficient of thermal expansion, and elastic modulus.

2. Methods

2.1. Experimental methods

In this investigation, EPON 828 (Hexion, Columbus, OH) which is a diglycidyl of bisphenol A (bisA) epoxide (Fig. 1a) was cured with three different amine curing agents. The three different curing agents examined are: EPIKURE™ W/Curing agent W (Miller-Stephenson, Danbury, Connecticut) which is diethyltoluenediamine (DETDA); 5-Amino-1,3,3-trimethylcyclohexanemethylamine (Sigma-Aldrich, St. Louis, MO), which is known as isophorone diamine (IPDA), and JEFFAMINE T-403 polyetheramine (Huntsman, The Woodlands, TX) which is characterized by repeating oxypropylene units in the backbone. While DETDA and IPDA are bifunctional primary amines, T403 is a trifunctional primary amine. DETDA is a low viscosity, aromatic curing agent used in filament winding of composites, casting, and tooling and provides a moderately high glass transition temperature (T_g) (Fig. 1b). IPDA is a low viscosity cycloaliphatic amine that, compared to aromatic amines, cures at lower temperatures and results in a lower T_g (Fig. 1c). IPDA is commonly used for small-medium sized castings, filament winding, and electrical and general laminating applications. It should be noted that IPDA consists of a primary aliphatic and cycloaliphatic amine functionality that allows for selective adduction with epoxy resin. T403 (where 403 stands for the average molecular weight of the molecule) is a low viscosity curing agent that has more reactivity than DETDA and IPDA and has a reduced carbonation tendency compared to other types of aliphatic amines, making it useful for large castings and filament wound composite structures. When cured with epoxides, T403 exhibits a high strain to failure due to the long chain distance between cross-link sites [22] and a lower T_g in comparison to DETDA and IPDA.

The mix ratios and the curing schedules for all the material systems are listed in Table 1. The mix ratios were calculated by equating the amine hydrogen equivalent weight (AHEW) and the epoxide equivalent weights (EEW) of the specific curing agents and bisphenol A epoxide respectively. The cure schedules were selected in a manner such that experimental comparisons to previously published data can be carried out [23–25].

The epoxy specimens were tested for T_g, mass density, coefficient of thermal expansions (CTEs) and tensile modulus of elasticity. Modulated differential scanning calorimetry (MDSC) was used to determine the T_g of the materials using a TA Instruments DSC Q2000 (New Castle, DE) running V24.11 Build 124 control and analysis software. Shavings of 6–8 mg were put in TA Tzero aluminum pans and sealed with Tzero lids. The temperature ramp rate was 3 °C/min with a modulation amplitude of 1 °C. Each specimen was tested with three ramps, and the inflection point [26] in each ramp was recorded as the T_g. The initial

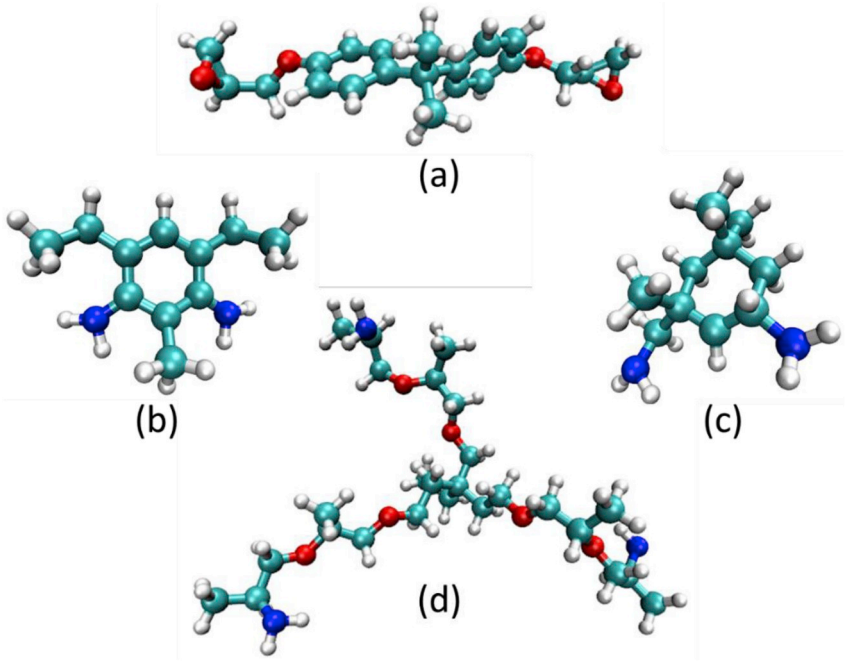

Fig. 1. Molecules examined for polymerization (a) bisphenol A, (b) diethyltoluenediamine (DETDA), (c) isophorone diamine (IPDA) and (d) JEFFAMINE T-403 polyetheramine. Cyan, red, blue and white spheres represent carbon, oxygen, nitrogen and hydrogen atoms respectively. (For interpretation of the references to colour in this figure legend, the reader is referred to the Web version of this article.)

Table 1
Mix ratios, nomenclature, and cure schedule for different material system examined.

Material System	Nomenclature (epoxide/curative)	Mix ratios (epoxide:curative)	Curing Schedule
Bisphenol A epoxide and diethyltoluenediamine	bisA/DETDA	100:23.3	3 h at 100 °C 2 h at 200 °C
Bisphenol A epoxide and isophorone diamine	bisA/IPDA	100:22.2	3 h at 100 °C 3 h at 125 °C
Bisphenol A epoxide and JEFFAMINE T-403 Polyetheramine	bisA/T403	100:42.9	24 h at 25 °C 3 h at 125 °C

Table 2
Temperature ranges for modulated differential scanning calorimetry (MDSC).

Material System	Initial – Final Temps. (°C)
bisA/DETDA	120–210
bisA/IPDA	100–160
bisA/T403	40–110

and final ramp temperatures for the different material systems are listed in Table 2.

ASTM D792-13 [27] was used for determining the mass density of the materials by the Archimedes method. As stipulated in "Method A" of the standard, de-ionized water was selected as the immersion medium. Five specimens of each type of material were used for measurement of mass density. The CTE was measured on a single specimen using resistance strain gages over a temperature range of 21–60 °C and the effects of transverse sensitivity in the gage measurements were eradicated using the procedure provided by Lanza di Scalea [28]. Tensile modulus was measured using a minimum of four dog bone specimens with two clip-gages on opposite sides of the specimen measuring average strain in the loading direction and one clip gage measuring strain in the transverse direction. A straight line was fit to the stress and strain data by the least square method over a longitudinal strain range of 500–3000 με to compute the modulus. A more detailed explanation of these matrix characterization details can be found in Vashisth et al. [5,29].

2.2. Computational details

ReaxFF is a reactive force field simulation procedure that is a bond order based molecular dynamics technique that considers the instantaneous interaction between atoms [17,30]. This strategy allows for smooth translation between non-bonded and bonded states that help to investigate the chemical reactions where bond formation and bond dissociation are involved during simulation. The contributing energies in ReaxFF are described by various contributions that can be summed up as:

$$E_{system} = E_{bond} + E_{over} + E_{under} + E_{val} + E_{angle} + E_{tors} + E_{vdW} + E_{Coulomb} + E_{lp} + E_{H\text{-}bond} + E_{rest} \quad (1)$$

where the total energy of the system (E_{system}) consists of bond energy (E_{bond}), over coordination (E_{over}), undercoordination (E_{under}), valence-angle energy (E_{val}), angle strain energy (E_{angle}), torsion angle energy (E_{tors}), van der Waals (E_{vdw}), Coloumb energy ($E_{Coulomb}$), lone pair energy (E_{lp}), hydrogen bond interactions ($E_{H\text{-}bond}$) and restrain energy (E_{rest}). Force field parameters used for ReaxFF are typically optimized by quantum mechanical (QM) calculations. A recent review paper by Senftle et al. [31] summerizes the capabilities and wide range of applications that have been successfully simulated using ReaxFF.

The external energy provided to the atoms during the accelerated simulations is given by the restrain energy term (E_{rest}). The total additional energy provided to the system is the sum of restrain energies provided to various pairs of atoms. Restrain energy (E_{rest}) for a pair of atoms is given by Equation (2),

$$E_{rest} = F_1\left\{1 - e^{-F_2(R_{ij}-R_{12})^2}\right\} \quad (2)$$

where F_1, F_2: Force parameters for restrain energy with units of kcal/mol and $Å^{-2}$, respectively; R_{12}: Target distance between two atoms according to restrain, in Å and R_{ij}: Actual distance between two atoms under consideration, in Å.

It is essential to choose the correct values of the restrain energy parameters which provide optimum energy for cross-linking. In addition, radial distribution (*rdf*) calculations were carried out for choosing the cut-off distances at a density of ~0.1 g/cc. A re-optimized version of the force field [21] based on the functionalized hydrocarbons/water weak interactions in condensed phase (CHNO-2017_weak) [32] was used for carrying out the accelerated simulations for epoxide-amine reactions.

2.3. Simulation procedure

2.3.1. Polymerization strategy

The accelerated ReaxFF simulations that provide extra energy to reactive sites is similar to the bond-boost method from Miron and Fichthorn [33]. In the ReaxFF accelerated approach, first the reacting atoms are identified when the specified cut-off ranges between multiple pairs of atoms are satisfied, and then their equilibrium configurations are determined. Whenever the spatial configurations of marked atoms are satisfied, additional energy will be provided to the reactants that is dependent on the chosen restrain energy parameters (F_1, F_2, and R_{12}). Next, an extra potential in terms of additional energy is added to these atoms during the standard MD simulations in the form of restrain energy (E_{rest}) Equation (2). It is ensured that the additional energy provided to the atoms is slightly larger than the barrier energy for polymerization. This additional energy provided to the atoms to stretch or compress the bonds aids the identified atoms for making or breaking of covalent bonds. In this investigation, the extra potentials (E_{rest}) are maintained for 10,000 time-steps of 0.25 fs whenever the spatial constraints are satisfied. It should be noted that not all accelerated cases lead to a successful reaction. In some cases, steric hindrance or the path approach is such that the additional energy provided to the system is not sufficient to drive the reactants to a transition structure that can form a stable product. Thus, in such cases, the reactants revert to their original molecular shape. The flowchart for the accelerated simulation to carry out polymerization between epoxide and amines is shown in Fig. 2. Amsterdam Density Function (ADF) [34] was used to simulate the accelerated ReaxFF.

The epoxide and the amine molecules for all the material systems were added in a manner such that a 1:1 stoichiometric ratio (one epoxide ring for each N—H) was maintained throughout the simulations. For bisA/DETDA and bisA/IPDA, the epoxide to amine ratio was 2:1 whereas for bisA/T403 the ratio was 3:1. The polymerization strategy was similar to that used in Ref. [21] where the number of molecules was doubled at every step. Accelerated NVT simulations were carried out at a temperature equal to the final cure stage and same force parameters were used for all the material systems. The force parameters

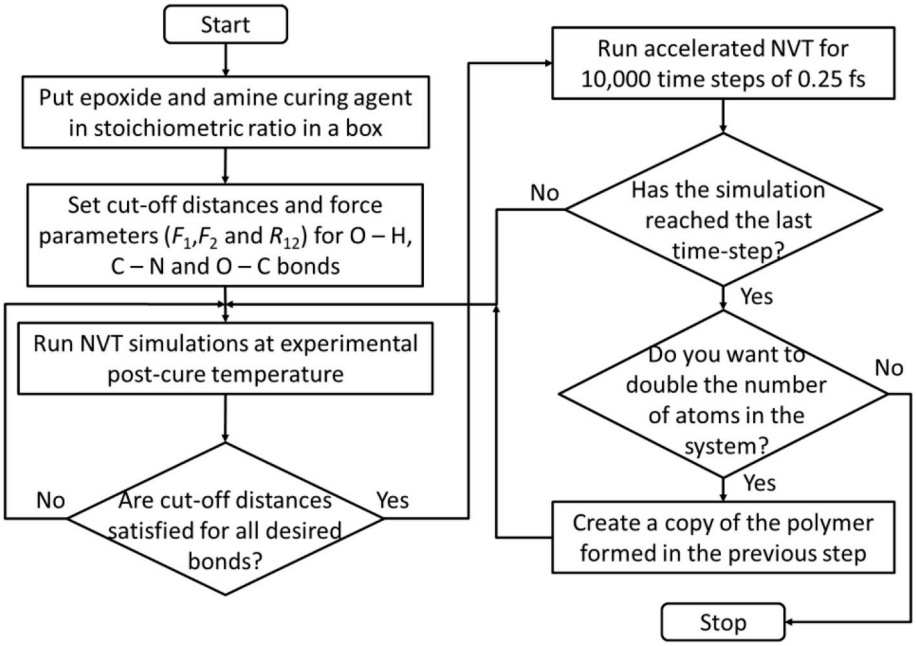

Fig. 2. Flowchart for accelerated simulations of epoxide and amine curing agents.

(R_{12}, F_1 and F_2) for bonds: O—C were 1.95 Å, 75 kcal/mol and 0.75 $Å^{-2}$; for O—H were 1.05 Å, 250 kcal/mol and 0.75 $Å^{-2}$; and for C—N were 1.5 Å, 300 kcal/mol and 0.75 $Å^{-2}$. All the reactions were carried out during NVT simulations using a Berendsen thermostat with a 100 fs temperature damping constant.

2.3.2. Polymer analysis

The polymer that was formed at the end of the simulations had local heterogeneities which were resolved by a repeated annealing process. Annealing was carried out by heating the polymer from 26.9 °C (300 K) to 326.9 °C (600 K) and then cooling it back to 26.9 °C (300 K). The temperatures were ramped by 100 °C increments, and then NPT simulation was carried out at the new temperature. Each NPT and NVT simulation was carried out for 12.5 ps with 0.25 fs timesteps. The Berendsen damping constants for thermostat in NVT simulation was 100 fs and the barostat for NPT was 500 fs For generating a density versus temperature graph, NPT calculations were carried out over a temperature range of 25 °C – 325 °C at an interval of 20 °C for 300,000 time-steps of 0.25 fs The glass transition temperature was calculated by finding the intersection of two straight lines fitted by linear regression to the density versus temperature results. For calculating the CTEs, NPT simulations at four temperatures — 26.9 °C (300 K), 36.9 °C (310 K), 46.9 °C (320 K) and 56.9 °C (330 K) — were carried out for 300,000 time-steps of 0.25 fs and the average strain in all three directions was used for calculating strain versus temperature dependence.

Previous studies have shown variation in modulus at such high strain rates [9]. Therefore, to simulate the modulus of the polymer, two strain rates were applied, namely 2×10^8 s^{-1} and 1×10^8 s^{-1}. It should be noted that experimental and simulation strain rates are drastically different and therefore multiple strain rates were considered in the experiments and simulations so that trend lines could be fitted to the results. The molecules were virtually tested in all three directions by changing the box size with the constraint that the box shape always remains cuboidal. The averages of these simulations are presented in the results. The four faces parallel to the strain direction were free to approach each other due to Poisson's effect. Large-scale Atomic/Molecular Massively Parallel Simulator (LAMMPS) [35] was used to simulate tensile testing with the “compute stress/atom command” [36] using a ReaxFF force field. Using these multiple points from experiments and simulations, a regression curve was plotted to examine the extrapolated modulus results.

3. Results and discussion

For running the accelerated ReaxFF, force parameters (mention in the previous section) and cut-off distances were required. The cut-off distances were determined using the radial distribution function (*rdf*) plots in Fig. 3, such that the ranges selected for O—H and C—N encompasses both the peaks. The O—C cut-off distance was selected to be between 1.3 Å – 1.60 Å such that only the closed epoxide rings are selected for accelerated simulations. It should be noted that increasing the upper limit of O—C cut-off distance can lead to unwanted reactions with open epoxide rings as well as the oxygen within the backbone of bisA structure. In this investigation, such reactions were neglected by being selective in choosing the O—C bond distances. The bond cutoff ranges for O—H and C—N for all the polymer systems were kept the same as 1.5 Å – 8.0 Å and 3.0 Å – 8.0 Å, respectively. The upper limits for cut-off distances of O—H and C—N can change the percentage cross-linking in the polymer as seen by Ref. [7]. The file used as input parameters for ReaxFF (tracking.in) can be found in the Supplementary Information.

Fig. 4 shows the polymerization sequence of bisA and DETDA starting with two molecules of bisA and one molecule of DETDA and doubling the number of molecules at every stage as defined in the schematic in Fig. 2. The final molecular structure of bisA/DETDA, bisA/IPDA and bisA/T403 consisted of 8256, 8384 and 7648 atoms, respectively. There are eight polymer chains of each material system in the final molecular structure. The final cross-linked densities of the polymers were 84%, 82% and 72%, respectively, which was calculated by dividing the number of C—N bonds formed by the possible C—N bonds. Bandyopadhyay et al., 2011 [7] concluded that significant changes in thermo-mechanical properties do not occur beyond a cross-linking density of ~75%.

After running a single NPT simulation of polymer, local heterogeneities were still present in the polymer. Therefore, three cycles of annealing were carried out to get convergence in the density of the polymer. The polymers formed at the end of the third annealing cycle (shown in Fig. 5) were used for thermo-mechanical virtual testing. Fig. 5 shows one of the faces for the cubic representative volume.

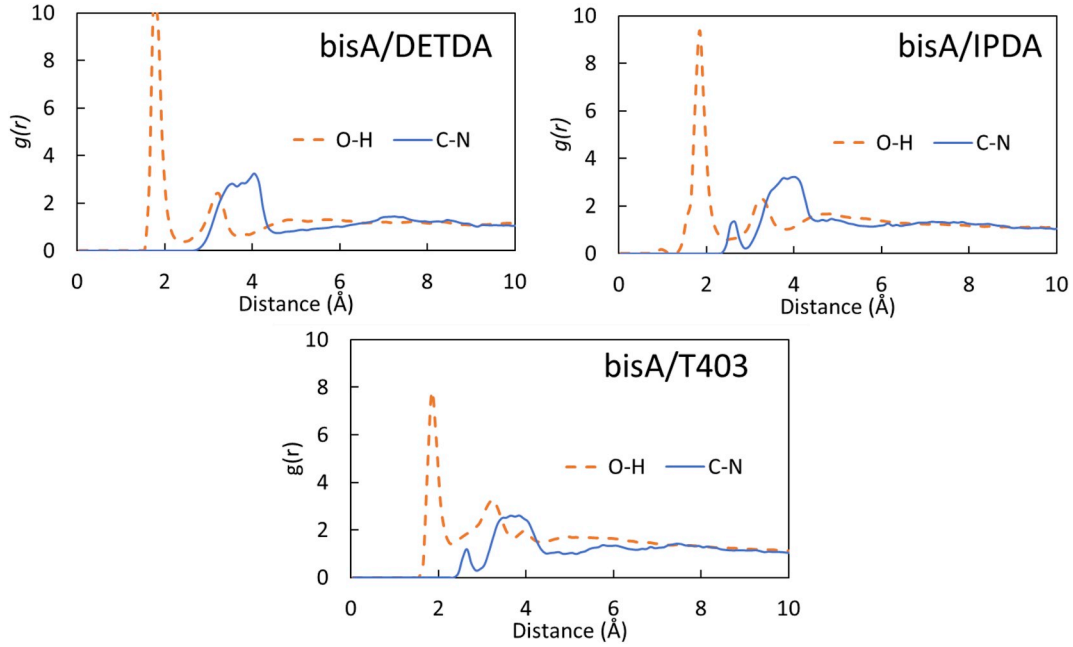

Fig. 3. Radial distribution function (*g(r)*) for O-H and C-N pair distances for three different material systems (bisA/DETDA, bisA/IPDA and bisA/T403).

On examining the annealing cycles (Fig. 6), it was observed that the bisA/DETDA and bisA/IPDA polymers had a low initial density to begin and a significant increase in density is observed at the end of the first annealing cycle. However, the density of bisA/T403 did not increase appreciably. This observation suggests more local heterogeneities in cyclic amines (aromatic and cyclo-aliphatic) as compared to aliphatic amines. Aliphatic amine molecules have less geometrical rigidity due to lack of rings, and also the aliphatic molecules used in this investigation are longer than the cyclic amines which allow them to branch and fill local voids in the structure, thereby having little local heterogeneities.

The simulated room-temperature densities of the final polymers are compared with the experimental results in Fig. 7. The density of each resin system was the average of all the time-steps of NPT simulations from the third annealing cycle. Good agreement is found between simulation and experiment densities. The differences between the simulations and experiments are 0.4%, 2.6% and 2.2% for bisA/DETDA, bisA/IPDA, and bisA/T403, respectively. A representative density versus temperature profile is provided in Supporting Information. Sindt et al. [37] reported 1.13 g/cc density for bisA/IPDA system, which is between the measured and simulated results obtained in this

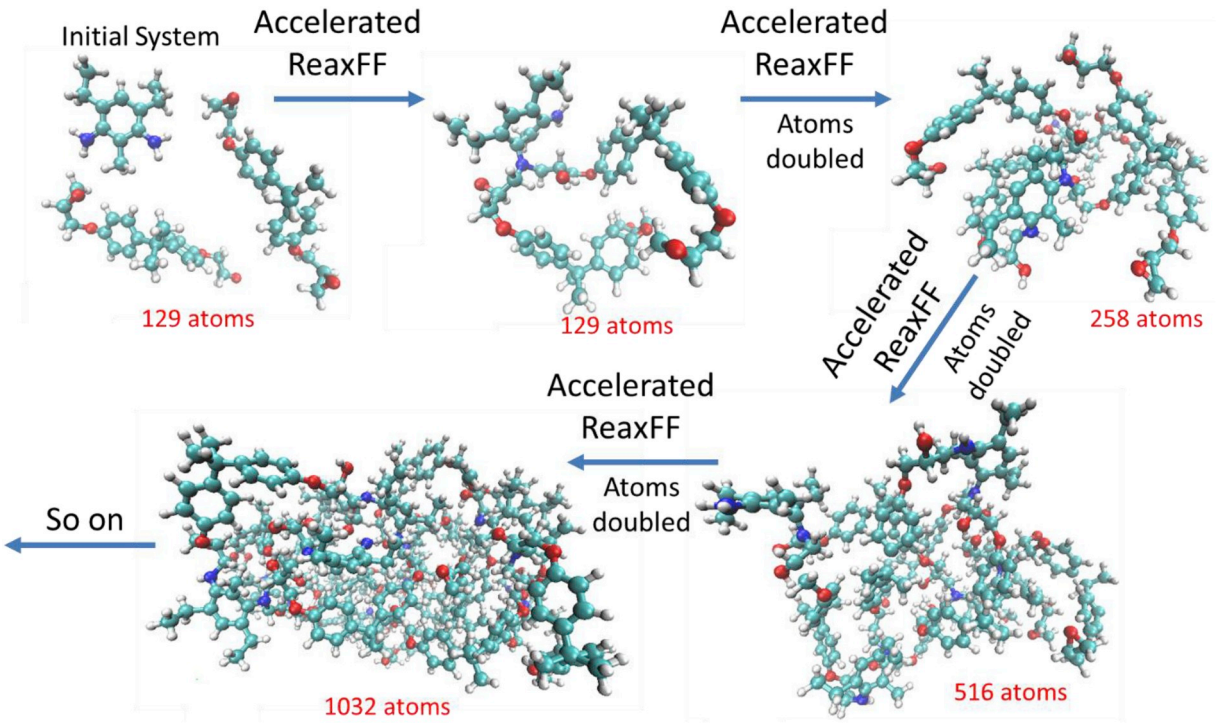

Fig. 4. Polymerization sequence of bisA/DETDA starting with an initial system with one DETDA and two bisA molecules.

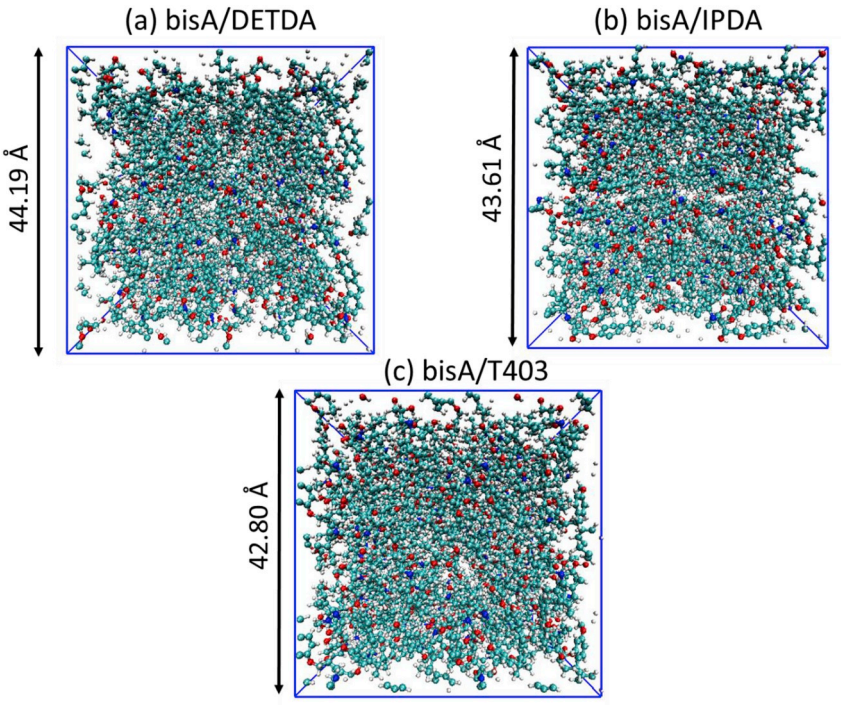

Fig. 5. Annealed structures of (a) bisA/DETDA (b) bisA/IPDA and (c) bisA/T403 used for thermo-mechanical testing. Cyan, red, blue and white spheres represent carbon, oxygen, nitrogen and hydrogen atoms respectively. (For interpretation of the references to colour in this figure legend, the reader is referred to the Web version of this article.)

investigation. Also, bisA/T403 epoxies cured at 125 °C [25] had a minimal difference of 4.7% as compared to density of bisA/T403 measured in the current study.

Fig. 8a shows that the simulated and measured T_g values are in close agreement and that the T_g results follow the expected trends for the three resin chemistries. Dynamic mechanical analysis performed by de Nograro et al. [38] determined the loss tangent T_g of the bisA/T403 system to be ~90 °C, which is 7 °C higher than the experimental T_g recorded in this investigation, potentially due to a higher post cure (at 180 °C) followed by Nograro et al. [38]. Another cause of difference can be variation in vendors for the chemicals. Norgraro et al. [38] also observed that the T_g increased on replacing aliphatic amines with aromatic amine curing agent. Similar trends were observed through experiments and replicated by ReaxFF simulations in this study. Shenogina et al. [39] simulated a T_g of 177–190 °C for ~90% cross-linked bisA/DETDA polymer and experimental investigation have measured T_g of 176 °C [40] and ~195 °C (using tan δ DMA) [23] for specimens post-cured at 200 °C. BisA/DETDA post-cured at 200 °C had a T_g of 176 °C as measured by Liu et al. [40] and the current investigation found a T_g of 178 °C using the DSC inflection point for specimens with similar post-cure.

Fig. 8b shows the experimental CTEs for three different resin

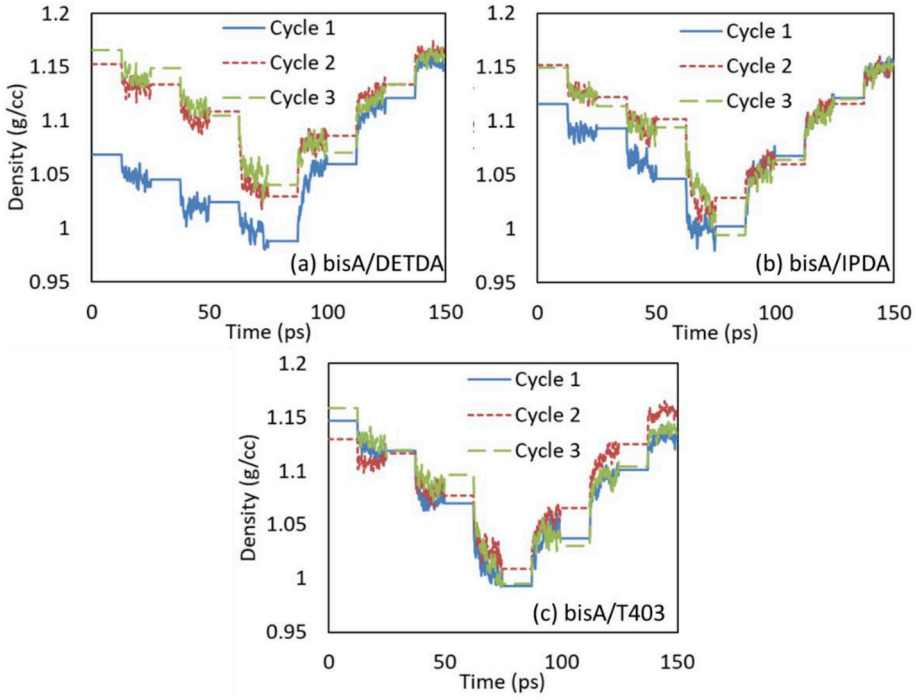

Fig. 6. Annealing cycles of polymers with different molecular chemistry: (a) bisA/DETDA; (b) bisA/IPDA and (c) bisA/T403.

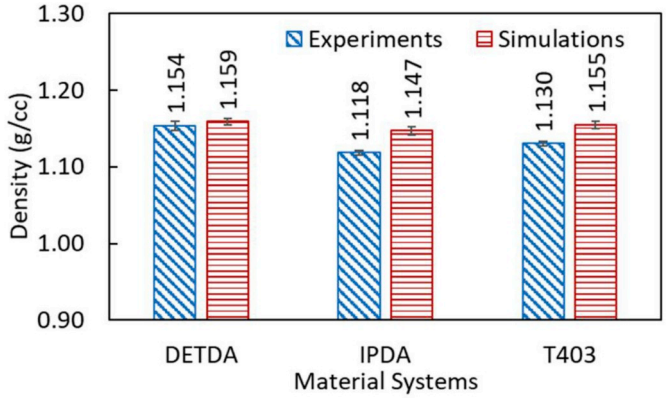

Fig. 7. Experimentally measured and simulated room-temperature density for bis A epoxide cured with DETDA, IPDA, and T403.

chemistries plotted along with the simulation results. The simulated CTEs show that the aliphatic curing agents provide slightly higher CTEs, presumably due to their higher mobility relative to the aromatic curing agent at the molecular scale. The experimental CTEs do not show significant differences between the different resin chemistries, considering the experimental scatter. Considering that the simulations under-predict the CTEs, further optimization of the force field may be required for more accurate predictions. Liu et al. [40] measured CTE of bisA/DETDA to be 65×10^{-6}/°C as compared to $(52.4 \pm 5.4) \times 10^{-6}$/°C measured in the current investigation. This difference of ~19% can result from different methods of CTE measurement, even though the post-cure temperatures were the same.

Fig. 9 shows the experimental and simulated elastic moduli plotted over the investigated strain rates. The modulus versus strain rate results were fitted with a linear regression curve, resulting in R^2 (coefficient of determination) values greater than 0.84. The simulated modulus results are also tabulated in the Supporting Information. While the modulus of aromatic and cyclo-aliphatic polymer changes by 31% and 40%, respectively, going from the smallest experimental strain rate to highest simulated strain rate, the change is 73% for the aliphatic polymer. This significant increase in modulus for aliphatic polymer chains as compared to aromatic and cycloaliphatic polymer can be attributed to longer aliphatic molecules that have a higher possibility of entanglement. The experimental and simulation values for density and T_g are listed in Table 3.

The experimental and simulation results for all the different chemistries examined in this investigation are listed in Table 4. For bisA/DETDA polymer, simulations have predicted a wide range of modulus (2.8–8.5 GPa) [39,42], while in the current investigation a range of 2.9–3.4 GPa was measured. Wu and Xu [14] found that simulated modulus of bisA/IPDA polymer network with up to 93.7% conversion was 5.2 GPa using COMPASS force field [41] and 47.2 GPa using Dreiding 2.21 force field [43]. These simulated moduli were higher than the experimental numbers [37]. Although, Wu and Xu [14] found

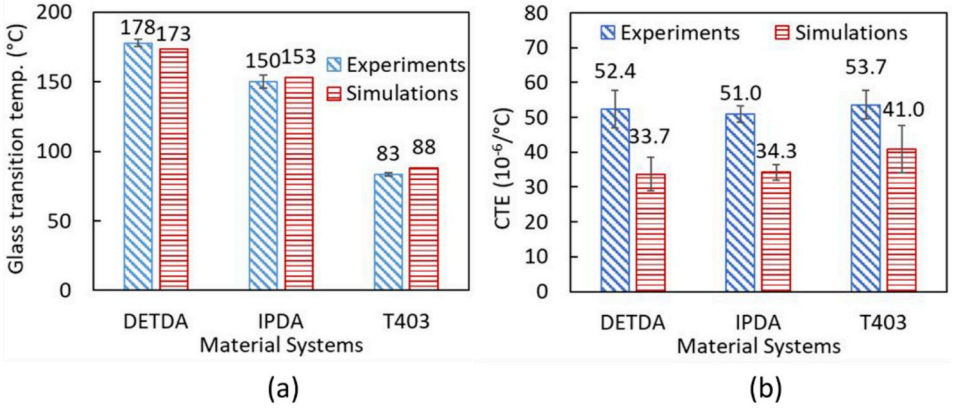

Fig. 8. (a) T_g results and (b) CTE results for all the resin system examined.

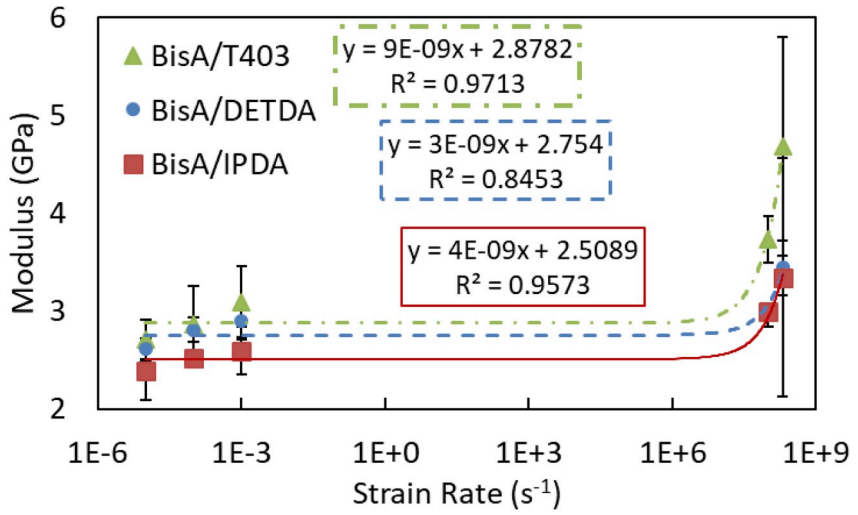

Fig. 9. Measured and simulated modulus for all resin systems (*x*-axis is logarithmic scale for strain rate).

Table 3
Tabulated data from experiments and simulations for glass transition temperature (T_g) and density (ρ) for different resin chemistries from literature and current investigation.

Material System	Sim. (Force Field)	Exp. (Cure Cycle)	Measured Property	Ref.	Note
BisA/DETDA	COMPASS	–	T_g: 177–190 °C	[39,41]	Coarse-grained method 90% cross-linking convergence
	–	2 h @ 100 °C 2 h @ 120 °C 4 h @ 175 °C 2 h @ 200 °C	T_g: 176 °C	[40]	Thermomechanical Analysis used for T_g. Similar post-cure as current investigation
	–	2 h @ 200 °C	T_g: ~195 °C	[23]	Using tan δ from DMA
	ReaxFF	–	T_g: 173 °C ρ: 1.16 g/cc	**Current Investigation**	
	–	3 h @ 100 °C 2 h @ 200 °C	T_g: 178 °C ρ: 1.15 g/cc		
BisA/IPDA	–	1 h @ 140 °C 6 h @ 190 °C	ρ: 1.131 g/cc T_g: 163 °C	[37]	High temperature post-cure as compared to current study
	ReaxFF	–	ρ: 1.15 g/cc T_g: 153 °C	**Current Investigation**	
	–	3 h @ 100 °C 3 h @ 125 °C	ρ: 1.12 g/cc T_g: 150 °C		
BisA/T403	—	2 h @ 80 °C 3 h @ 125 °C	ρ: 1.07 g/cc T_g: 96 °C	[25]	Similar post-cure as current investigation
	ReaxFF	–	ρ: 1.16 g/cc T_g: 88 °C	**Current Investigation**	
	–	24 h @ 25 °C 3 h @ 125 °C	ρ: 1.12 g/cc T_g: 83 °C		

good agreement between simulations with the experimental results from Ref. [37] – density (1.131 g/cc), T_g (163 °C) and modulus (4.71 GPa) – were significantly higher than that measured in this study. This can be attributed to the fact that specimens in Ref. [37] were post-cured at much higher temperatures as compared to this study.

Nograro et al. [38] measured a flexural modulus of ~3.25 GPa for bisA/T403 at strain rates of $\sim 3 \times 10^{-4}$ ε/s, while the current investigation found the experimental modulus to be 3.09 ± 0.38 GPa at 1×10^{-4} ε/s. Burton et al., 2005 [25] reported modulus and the T_g of 2.88 GPa and 96 °C for bisA/T403 with similar post cure as the current investigation. These experimental results from Burton et al. [25] are in good agreement with the experimental observations of the current study.

The crosslinking predicted is different for three different chemistries using the same "Accelerated ReaxFF" parameters, with the lowest crosslinking for T403 curative suggesting limited accessibility of the $-NH_2$ attached to an aliphatic chain. The backbone structure of the curative influences the thermo-mechanical properties of the epoxy, but the effect is manifested most prominently in T_g. As T_g marks the onset of the molecular motion, various factors can potentially affect the movement of the polymer chain thereby influencing T_g. These include chain flexibility, molecular structure as well as crosslinking.

Chain flexibility depends more on the rotation or torsion of skeletal bonds (which would influence the dihedrals) than on changes in the bond angles. When a randomly coiled chain is pulled out into an elongated conformation, the skeletal bonds unwind rather than going through angular distortion (See Figure S2). Thus, flexibility on a macroscopic scale depends on torsional mobility at molecular level [45,46]. A highly flexible chain results in a lower T_g whereas a rigid chain results in a higher T_g. The chemical structural nature of the backbone chain is

Table 4
Tabulated data from experiments and simulations for tensile modulus from literature and current investigation.

Material System	Sim. (Force Field)	Exp. (Cure Cycle)	Modulus (GPa)	Ref.	Note
BisA/DETDA	AMBER	–	2.8	[42]	80% cross-linking convergence
	COMPASS	–	5.5–8.5	[39,41]	Coarse-grained method 90% cross-linking convergence
	–	2 h @ 179 °C	2.71	[44]	ASTM D638-99 used for measuring E
	ReaxFF	–	2.9–3.44	**Current Investigation**	
	–	3 h @ 100 °C 2 h @ 200 °C	2.6–2.9		
BisA/IPDA	COMPASS	–	5.2	[14]	93.7% conversion
	Dreiding 2.21	–	47.2		
	–	1 h @ 140 °C 6 h @ 190 °C	4.71	[37]	High temperature post-cure
		3 h @ 100 °C 3 h @ 125 °C	3.25	[24]	Similar cure cycle as this investigation
	ReaxFF	–	3.0–3.4	**Current Investigation**	
	–	3 h @ 100 °C 3 h @ 125 °C	2.4–2.6		
BisA/T403	—	3 h @ 70 °C 2 h @ 180 °C	~3.25	[38]	strain rates: $\sim 3 \times 10^{-4}$ ε/s
		2 h @ 80 °C 3 h @ 125 °C	2.88	[25]	Similar post-cure to this investigation
	ReaxFF	–	3.7–4.7	**Current Investigation**	
	–	24 h @ 25 °C 3 h @ 125 °C	2.7–3.1		

also an essential factor determining the chain flexibility and hence the T_g. Chains that consist of flexible sequences (such as $-CH_2-CH_2-$ or $-CH_2-O-CH-$ in aliphatic T403) can rotate easily, therefore resulting in low T_g. While the T_g improves significantly by insertion of groups that stiffen the chain by impeding rotational motion so that more thermal energy is required to set the chain in motion [46]. Therefore, due to chain flexibility and molecular structure, T_g of bisA/DETDA should be the highest as it has rigid benzene rings, followed by bisA/IPDA that has cycloaliphatic rings and finally bisA/T403 with linear chains. These molecular mechanisms are captured by the simulations correctly as the experiments and the simulations correlate well for T_g calculations. The terms E_{tors} and E_{val}, which contribute to the total energy of the system in Equation (1), account for the torsional and angle energies for each dihedral and bond angle, including those in the benzene, cyclic and linear chains of DETDA, IPDA and T403 structures, respectively.

Elevated temperatures result in increased kinetic energy which contributes to higher velocities for atoms. Higher atom velocities cause bond extensions, twists in valence and torsion angles that are manifested in the E_{val} and E_{tor} energy terms in ReaxFF. A more stable molecular chain has less contribution to E_{val} and E_{tor} and therefore has less mobility on being provided more thermal energy. On heating the simulated polymers to 46.9 °C (320 K), the E_{val} terms in bisA/DETDA, bisA/IPDA and bisA/T403 systems account for 5.23%, 5.39% and 5.52% of the total energy, respectively, whereas the E_{tor} terms account for 1.12%, 1.18% and 1.18% of the total energy, respectively. These considerations suggest higher mobility of the polymer chains in the T403 system as compared to the IPDA and DETDA systems.

Another factor influencing T_g is crosslinking density, which was simulated to be 84%, 82% and 72% for bisA/DETDA, bisA/IPDA and bisA/T403, respectively, using a single set of "Accelerated ReaxFF" parameters. When two polymers are connected by introducing a crosslink, the polymer chains are pulled together at these points and the free volume is decreased. This reduction in free volume results in increased T_g. Therefore, if we ignore the other factors influencing T_g, crosslinking density simulated by "Accelerated ReaxFF" suggests that the DETDA and IPDA systems should have a higher T_g as compared to the T403 system.

The three factors discussed above—chain flexibility, molecular structure, and crosslinking—also influence the CTEs. A more flexible, less rigid and less cross-linked chain expands more when thermal energy is provided to the polymer, resulting in higher CTE [45]. This is observed from the simulation results where the CTE of bisA/T403 is greater than bisA/DETDA and bisA/IPDA. Simulations on Bisphenol F and DETDA with varying degree of crosslinking indicate that the CTEs decreases with overall crosslink density [47].

Although the reactive sites are the same (epoxide ring and the amine) for all the molecular species examined in this investigation, the bond angles and dihedrals for the amine with the backbone structure are different, which potentially causes the barrier energies to change slightly. It should be noted that accelerated ReaxFF accounts for minor changes in the barrier energies. A more detailed quantum mechanical study is required to find barrier energies for amines on aliphatic, cycloaliphatic and aromatic backbones that can be used to generate force field to refine the cross-linking accelerated ReaxFF simulations.

4. Conclusions

A newly developed method to simulate reactions with slow kinetics was developed within the framework of ReaxFF was used to simulate polymerization of bisphenol A epoxide with aromatic, cyclo-aliphatic and aliphatic amine curing agents. The polymers formed were then analyzed for thermo-mechanical properties, and a good agreement between the experiments and the simulations was observed. It was also seen that simulated polymers with cyclic amine (aromatic and cycloaliphatic) had more local heterogeneities as compared to aliphatic amines. An annealing process was employed to eliminate these local heterogeneities. The mechanical response of the polymer showed that cyclic amines were less affected by higher strain rates as compared to aliphatic amines. The glass transition temperatures were in good agreement with the experiments, whereas the simulated coefficients of thermal expansion were systematically lower than the experimental results. Using the developed tools, the thermo-mechanical properties of epoxies manufactured with different monomers can be examined. As these properties are controlled by the molecular architecture, by varying the curing temperature and additional energy (E_{rest}) provided for accelerated ReaxFF, simulations can help in replicating the properties of different polymers that were cured at a different temperature. Another interesting application is the use of the virtually cross-linked polymers for virtual testing under different regimes such as modulus at different strain rates, densities at different temperatures, different water contents, etc. To further improve the comparisons between experiments and simulations, curing of the epoxy can be experimentally monitored during the polymerization reaction using infrared (IR) [48,49] or dielectric spectroscopy [50,51]. This could help in targeting the exact percentage cure for when simulating a particular reaction. Also, the newly developed accelerated ReaxFF can be further refined by incorporating angular and dihedral constraints that potentially play a role in the polymerization.

Acknowledgments

The Institute for Cyberscience at Penn State is acknowledged for seed funding. This research is partially funded by the Government under Agreement No. W911W6-11-2-0011. The U.S. Government is authorized to reproduce and distribute reprints notwithstanding any copyright notation thereon. The views and conclusions contained in this document are those of the authors and should not be interpreted as representing the official policies, either expressed or implied, of the U.S. Government.

Appendix A. Supplementary data

Supplementary data to this article can be found online at https://doi.org/10.1016/j.polymer.2018.11.005.

References

[1] C. May, Epoxy Resins: Chemistry and Technology, CRC press, 1987.
[2] B. Ellis, M.S. Found, J.R. Bell, Influence of cure treatment on extent of reaction and glassy modulus for BADGE-DDM epoxy resin, J. Appl. Polym. Sci. 82 (2001) 1265–1276, https://doi.org/10.1002/app.1960.
[3] A.T. Detwiler, A.J. Lesser, Aspects of network formation in glassy thermosets, J. Appl. Polym. Sci. 117 (2010) 1021–1034, https://doi.org/10.1002/app.31681.
[4] E. Morel, V. Bellenger, M. Bocquet, J. Verdu, Structure-properties relationships for densely cross-linked epoxide-amine systems based on epoxide or amine mixtures, J. Mater. Sci. 24 (1989) 69–75, https://doi.org/10.1007/BF00660934.
[5] A. Vashisth, C.E. Bakis, Characterization of nanosilica filled bis F epoxide with diamino diphenyl sulfone curing agents, 31st Tech. Conf. Am. Soc. Compos, Destech Publications, Williamsburg, VA, 2016, p. 15.
[6] P.-H. Lin, R. Khare, Molecular simulation of cross-linked epoxy and Epoxy − POSS nanocomposite, Macromolecules 42 (2009) 4319–4327, https://doi.org/10.1021/ma9004007.
[7] A. Bandyopadhyay, P.K. Valavala, T.C. Clancy, K.E. Wise, G.M. Odegard, Molecular modeling of crosslinked epoxy polymers: the effect of crosslink density on thermomechanical properties, Polymer (Guildf) 52 (2011) 2445–2452, https://doi.org/10.1016/j.polymer.2011.03.052.
[8] I. Yarovsky, E. Evans, Computer simulation of structure and properties of cross-linked polymers: application to epoxy resins, Polymer (Guildf) 43 (2002) 963–969, https://doi.org/10.1016/S0032-3861(01)00634-6.
[9] C. Li, A. Strachan, Molecular dynamics predictions of thermal and mechanical properties of thermoset polymer EPON862/DETDA, Polymer (Guildf) 52 (2011) 2920–2928, https://doi.org/10.1016/j.polymer.2011.04.041.
[10] M.J. Stevens, Manipulating connectivity to control fracture in network polymer adhesives, Macromolecules 34 (2001) 1411–1415, https://doi.org/10.1021/ma0009505.
[11] S.J. Marrink, H.J. Risselada, S. Yefimov, D.P. Tieleman, A.H. de Vries, The MARTINI force field: coarse grained model for biomolecular simulations, J. Phys. Chem. B 111 (2007) 7812–7824, https://doi.org/10.1021/jp071097f.

[12] A.F. Voter, Introduction to the kinetic Monte Carlo method, in: Radiat. Eff. Solids, Springer Netherlands, Dordrecht, n.d: pp. 1–23. doi:10.1007/978-1-4020-5295-8_1.
[13] D.R. Heine, G.S. Grest, C.D. Lorenz, M. Tsige, M.J. Stevens, Atomistic simulations of end-linked poly(dimethylsiloxane) networks: structure and relaxation, Macromolecules 37 (2004) 3857–3864, https://doi.org/10.1021/ma035760j.
[14] C. Wu, W. Xu, Atomistic molecular modelling of crosslinked epoxy resin, Polymer (Guildf) 47 (2006) 6004–6009, https://doi.org/10.1016/j.polymer.2006.06.025.
[15] V. Varshney, S.S. Patnaik, A.K. Roy, B.L. Farmer, A molecular dynamics study of epoxy-based networks: cross-linking procedure and prediction of molecular and material properties, Macromolecules 41 (2008) 6837–6842, https://doi.org/10.1021/ma801153e.
[16] C. Li, A. Strachan, Molecular simulations of crosslinking process of thermosetting polymers, Polymer (Guildf). 51 (2010) 6058–6070, https://doi.org/10.1016/j.polymer.2010.10.033.
[17] A.C.T. Van Duin, S. Dasgupta, F. Lorant, W.A. Goddard, ReaxFF: a reactive force field for hydrocarbons, J. Phys. Chem. 105 (2001) 9396–9409, https://doi.org/10.1021/jp004368u.
[18] S.J. Stuart, A.B. Tutein, J.A. Harrison, A reactive potential for hydrocarbons with intermolecular interactions, J. Chem. Phys. 112 (2000) 6472–6486, https://doi.org/10.1063/1.481208.
[19] D.W. Brenner, O.A. Shenderova, J.A. Harrison, S.J. Stuart, B. Ni, S.B. Sinnott, A second-generation reactive empirical bond order (REBO) potential energy expression for hydrocarbons, J. Phys. Condens. Matter 14 (2002) 783 http://stacks.iop.org/0953-8984/14/i=4/a=312.
[20] M.S. Radue, B.D. Jensen, S. Gowtham, D.R. Klimek-McDonald, J.A. King, G.M. Odegard, Comparing the mechanical response of di-, tri-, and tetra-functional resin epoxies with reactive molecular dynamics, J. Polym. Sci., Part B: Polym. Phys. 56 (2018) 255–264, https://doi.org/10.1002/polb.24539.
[21] A. Vashisth, C. Ashraf, W. Zhang, C.E. Bakis, A.C.T. Van Duin, Accelerated ReaxFF simulations for describing the reactive cross-linking of polymers, J. Phys. Chem. 122 (2018) 6633–6642, https://doi.org/10.1021/acs.jpca.8b03826.
[22] W.R. Ashcroft, Curing agents for epoxy resins, Chem. Technol. Epoxy Resins, Springer Netherlands, Dordrecht, 1993, pp. 37–71, , https://doi.org/10.1007/978-94-011-2932-9_2.
[23] D. Ratna, R. Varley, R.K.S. Raman, G.P. Simon, Studies on blends of epoxy-functionalized hyperbranched polymer and epoxy resin, J. Mater. Sci. 38 (2003) 147–154, https://doi.org/10.1023/A:1021182320285.
[24] J.-L. Tsai, B.-H. Huang, Y.-L. Cheng, Enhancing fracture toughness of glass/epoxy composites by using rubber particles together with silica nanoparticles, J. Compos. Mater. 43 (2009) 3107–3123, https://doi.org/10.1177/0021998309345299.
[25] B. Burton, D. Alexander, H. Klein, A. Garibay-Vasquez, A. Pekarik, C. Henkee, Epoxy formulations using Jeffamine® polyetheramines, huntsman service, http://www.huntsman.com/performance_products/Media%20Library/global/files/epoxy_formulations_using_jeffamine_polyetheramines.pdf, (2005).
[26] ASTM Standard D 1356 - 08, Standard Test Method for Assignment of the Glass Transition Temperatures by Differential Scanning Calorimetry, (2014), pp. 1–4.
[27] ASTM D792 - 13, Standard Test Methods for Density and Specific Gravity (Relative Density) of Plastics by Displacement, (2013), p. 6, https://doi.org/10.1520/d0792.
[28] F. Lanza di Scalea, Measurement of thermal expansion coefficients of composites using strain gages, Exp. Mech. 38 (1998) 233–241, https://doi.org/10.1007/BF02410384.
[29] A. Vashisth, Multi-scale Characterization and Modelling of Nanosilica Reinforced Carbon/Epoxy Composites for Filament Wound Structures, The Pennsylvania State University, 2018.
[30] K. Chenoweth, A.C.T. van Duin, W. a Goddard, ReaxFF reactive force field for molecular dynamics simulations of hydrocarbon oxidation, J. Phys. Chem. 112 (2008) 1040–1053, https://doi.org/10.1021/jp709896w.
[31] T.P. Senftle, S. Hong, M.M. Islam, S.B. Kylasa, Y. Zheng, Y.K. Shin, C. Junkermeier, R. Engel-Herbert, M.J. Janik, H.M. Aktulga, T. Verstraelen, A. Grama, A.C.T. van Duin, The ReaxFF reactive force-field: development, applications and future directions, NPJ Comput. Mater. 2 (2016) 15011, https://doi.org/10.1038/npjcompumats.2015.11.
[32] W. Zhang, A.C.T. van Duin, Improvement of the ReaxFF description for functionalized hydrocarbon/water weak interactions in the condensed phase, J. Phys. Chem. B (2018), https://doi.org/10.1021/acs.jpcb.8b01127 acs.jpcb.8b01127.
[33] R.A. Miron, K.A. Fichthorn, Accelerated molecular dynamics with the bond-boost method, J. Chem. Phys. 119 (2003) 6210–6216, https://doi.org/10.1063/1.1603722.
[34] E.J. Baerends, T. Ziegler, A.J. Atkins, J. Autschbach, D. Bashford, O. Baseggio, A. Bérces, F.M. Bickelhaupt, C. Bo, P.M. Boerritger, L. Cavallo, C. Daul, D.P. Chong, D. V Chulhai, L. Deng, R.M. Dickson, J.M. Dieterich, D.E. Ellis, M. van Faassen, A. Ghysels, A. Giammona, S.J.A. van Gisbergen, A. Goez, A.W. Götz, S. Gusarov, F.E. Harris, P. van den Hoek, Z. Hu, C.R. Jacob, H. Jacobsen, L. Jensen, L. Joubert, J.W. Kaminski, G. van Kessel, C. König, F. Kootstra, A. Kovalenko, M. Krykunov, E. van Lenthe, D.A. McCormack, A. Michalak, M. Mitoraj, S.M. Morton, J. Neugebauer, V. P. Nicu, L. Noodleman, V.P. Osinga, S. Patchkovskii, M. Pavanello, C.A. Peeples, P. H.T. Philipsen, D. Post, C.C. Pye, H. Ramanantoanina, P. Ramos, W. Ravenek, J.I. Rodríguez, P. Ros, R. Rüger, P.R.T. Schipper, D. Schlüns, H. van Schoot, G. Schreckenbach, J.S. Seldenthuis, M. Seth, J.G. Snijders, M. Solà, S. M., M. Swart, D. Swerhone, G. te Velde, V. Tognetti, P. Vernooijs, L. Versluis, L. Visscher, O. Visser, F. Wang, T.A. Wesolowski, E.M. van Wezenbeek, G. Wiesenekker, S.K. Wolff, T.K. Woo, A.L. Yakovlev, ADF2017, SCM, Theoretical Chemistry, Vrije Universiteit, Amsterdam, The Netherlands, https://www.scm.com, (n.d.).
[35] S. Plimpton, Fast parallel algorithms for short-range molecular dynamics, J. Comput. Phys. 117 (1995) 1–19, https://doi.org/10.1006/jcph.1995.1039.
[36] T.W. Sirk, S. Moore, E.F. Brown, Characteristics of thermal conductivity in classical water models, J. Chem. Phys. 138 (2013) 064505, https://doi.org/10.1063/1.4789961.
[37] O. Sindt, J. Perez, J.F. Gerard, Molecular architecture-mechanical behaviour relationships in epoxy networks, Polymer. 37 (1996) 2989–2997, https://doi.org/10.1016/0032-3861(96)89396-7.
[38] F.F. de Nograro, R. Llano-Ponte, I. Mondragon, Dynamic and mechanical properties of epoxy networks obtained with PPO based amines/mPDA mixed curing agents, Polymer (Guildf). 37 (1996) 1589–1600, https://doi.org/10.1016/0032-3861(96)83707-4.
[39] N.B. Shenogina, M. Tsige, S.S. Patnaik, S.M. Mukhopadhyay, Molecular modeling approach to prediction of thermo-mechanical behavior of thermoset polymer networks, Macromolecules 45 (2012) 5307–5315, https://doi.org/10.1021/ma3007587.
[40] W. Liu, R.J. Varley, G.P. Simon, Phosphorus-containing diamine for flame retardancy of high functionality epoxy resins. Part II. The thermal and mechanical properties of mixed amine systems, Polymer (Guildf) 47 (2006) 2091–2098, https://doi.org/10.1016/j.polymer.2005.12.083.
[41] H. Sun, COMPASS: an ab initio force-field optimized for condensed-phase Applications overview with details on alkane and benzene compounds, J. Phys. Chem. B 102 (1998) 7338–7364, https://doi.org/10.1021/jp980939v.
[42] T.C. Clancy, S.J.V. Frankland, J.A. Hinkley, T.S. Gates, Molecular modeling for calculation of mechanical properties of epoxies with moisture ingress, Polymer (Guildf) 50 (2009) 2736–2742, https://doi.org/10.1016/j.polymer.2009.04.021.
[43] S.L. Mayo, B.D. Olafson, W.A. Goddard, DREIDING: a generic force field for molecular simulations, J. Phys. Chem. 94 (1990) 8897–8909, https://doi.org/10.1021/j100389a010.
[44] B. Qi, Q.X. Zhang, M. Bannister, Y.W. Mai, Investigation of the mechanical properties of DGEBA-based epoxy resin with nanoclay additives, Compos. Struct. 75 (2006) 514–519, https://doi.org/10.1016/j.compstruct.2006.04.032.
[45] M. Rubinstein, R.H. Colby, Polymer Physics vol. 23, Oxford University Press, Inc., New York, 2003.
[46] M. Chanda, Advanced Polymer Chemistry. A Problem Solving Guide, Marcel Dekker, Inc., New York, 2000.
[47] A. Bandyopadhyay, G.M. Odegard, Molecular modeling of crosslink distribution in epoxy polymers, Model. Simulat. Mater. Sci. Eng. 20 (2012) 045018, https://doi.org/10.1088/0965-0393/20/4/045018.
[48] M.A. Acitelli, R.B. Prime, E. Sacher, Kinetics of epoxy cure: (1) the system bisphenol-A diglycidyl ether/m-phenylene diamine, Polymer (Guildf) 12 (1971) 335–343, https://doi.org/10.1016/0032-3861(71)90056-5.
[49] D.J. Plazek, Z.N. Frund, Epoxy resins (DGEBA): the curing and physical aging process, J. Polym. Sci., Part B: Polym. Phys. 28 (1990) 431–448, https://doi.org/10.1002/polb.1990.090280401.
[50] B.D. Fitz, J. Mijovic, Segmental dynamics and density fluctuations in polymer networks during chemical vitrification, Macromolecules 32 (1999) 4134–4140, https://doi.org/10.1021/ma981435y.
[51] G. Levita, A. Livi, P.A. Rolla, C. Culicchi, Dielectric monitoring of epoxy cure, J. Polym. Sci., Part B: Polym. Phys. 34 (1996) 2731–2737, https://doi.org/10.1002/(SICI)1099-0488(19961130)34:16<2731::AID-POLB6>3.0.CO;2-S.